

Film morphology and photophysics of polyfluorene

A. J. Cadby, P. A. Lane, H. Mellor, S. J. Martin, M. Grell, C. Giebeler, and D. D. C. Bradley
Department of Physics and Astronomy, University of Sheffield, Sheffield S3 7RH, United Kingdom

M. Wohlgenannt, C. An, and Z. V. Vardeny
Department of Physics, University of Utah, Salt Lake City, Utah 84112
(Received 10 September 1999; revised manuscript received 14 August 2000)

We have studied the interplay between photophysics and film morphology of poly(9,9-dioctyl)fluorene (PFO) using a variety of optical probes. Upon slowly warming a spin-cast PFO film from 80 to 300 K, a fraction of the sample is transformed into a different solid phase, the β phase. Absorption and electroabsorption measurements show that the β phase has more extended conjugation than the glassy phase. As a consequence, excited states of the β phase are redshifted and have higher polarizability. The photoinduced absorption spectrum of a glassy PFO film is dominated by triplet excitons, whereas both polarons and triplet excitons are seen in a sample containing a fraction of the β phase. The dependence of the photoinduced absorption and photocurrent upon the excitation wavelength shows that there is a clear link between polaron and triplet photogeneration.

I. INTRODUCTION

Polyfluorene has emerged as an attractive material for display applications owing to efficient blue emission¹ and hole mobility greater than $3 \times 10^{-4} \text{ cm}^2/\text{Vs}$ with trap-free transport.² Poly(9,9-dioctylfluorene) (PFO) has also been found to exhibit a complex morphological behavior that has interesting implications for its photophysical properties. In the melt, polyfluorenes show liquid crystalline phases that can be aligned and quenched into the glassy state, which has led to the fabrication of highly polarized electroluminescence devices.^{3,4} Two previous examples of harnessing structural versatility to manipulate electronic and optical properties in PFO are the observation of fast hole transport in glassy liquid crystalline monodomains⁵ and the variation of lasing properties with phase morphology.⁶

PFO films display different forms of (para)crystalline order. Spin-coating a PFO film from solution produces a glassy sample with spectroscopic characteristics typical of conjugated polymers. A different phase that has been called the β phase has been detected upon cooling a glassy film on a substrate to 80 K and slowly reheating it to room temperature or exposing a film to the vapor of a solvent or swelling agent.^{7,8} The spectroscopic properties of the glassy and β phases differ characteristically from one another. The π - π^* transition of the glassy phase is featureless, with a maximum at 3.23 eV (384 nm). Remarkably, the β phase shows a narrow, well resolved absorption peak at 2.84 eV (437 nm) and an associated vibronic structure superimposed upon the bulk absorption.^{7,8} This behavior has been correlated with the degree of intrachain ordering in the different phases. X-ray fiber diffraction measurements of the glassy phase have shown that the parallel-to-chain coherence length matches the length of persistence in solution⁸ ($85 \pm 10 \text{ \AA}$) as well as the effective conjugation length in solution.⁹ Hence, the effective conjugation length in glassy PFO is conformationally limited. The intrachain correlation length of the β phase is much longer (220 \AA). The observed redshift of absorption is

much longer than can be accounted for by extrapolation of a series of oligofluorenes to infinite conjugation length.⁹ It has therefore been proposed that mechanical stresses during β phase formation result in additional planarization.⁸ This proposal is supported by similarities in the photophysics of β phase PFO and planarized ladder-type poly(*para*-phenylene) (LPPP) that are described in this paper.

The rich phase morphology of PFO provides a unique opportunity to study the influence of film morphology on the photophysics of conjugated polymers without the need for chemical modification. The electronic structure of PFO films was studied by absorption, photoluminescence (PL), and electroabsorption spectroscopy. Photoexcitation dynamics were studied by photoinduced absorption (PA) spectroscopy. Triplet and charge photogeneration were studied by measuring the PA and photocurrent action spectra. The following sections describe the experimental techniques, studies of the electronic structure of PFO, and photoexcitation dynamics.

II. EXPERIMENTAL METHOD

The synthesis and characterization of PFO have been previously described.^{1,10,11} PFO has an ionization potential of 5.8 eV,¹² and an optical gap of 3.0 eV. For optical measurements, samples of PFO were spin-coated onto synthetic quartz (Spectrosil B) disks from toluene solution. The solutions were filtered prior to spin coating. Absorption spectra were measured in a Unicam UV-visible spectrophotometer. PL emission was collected with an optical fiber, dispersed in a spectrograph, and recorded with an Oriel charge-coupled device detector. For this measurement, samples were excited by a monochromated 150 W xenon arc lamp. Absorption and luminescence measurements were performed in an ambient environment at 300 K.

The electronic structure of polyfluorene films was investigated by absorption and electroabsorption (EA) spectroscopy.

copy. EA spectroscopy is an attractive nonlinear optical technique as it can be performed over a wide spectral range using continuous wave light sources. A sinusoidal electric field is applied to the sample to modulate its optical absorption. For nondegenerate states and to second order in the applied electric field, the result is a change in the optical absorption proportional to a combination of the first and second derivatives of the absorption coefficient with respect to energy. These arise from differences in the polarizability ($\partial\alpha/\partial E$) and/or permanent dipole moment ($\partial^2\alpha/\partial E^2$) of the ground and excited states.¹³ The electric field also mixes electronic states, which results in a transfer of oscillator strength from the strongly allowed to forbidden optical transitions. The transfer of oscillator strength results in a bleaching of the allowed absorption together with the appearance of induced absorption bands. The EA spectrum can be simulated by Eq. (1):

$$\Delta\alpha = c\alpha + \frac{1}{2}\Delta p F^2 \frac{\partial\alpha}{\partial E} + \frac{1}{6}(m_f F)^2 \frac{\partial^2\alpha}{\partial E^2} + \alpha', \quad (1)$$

where Δp is the difference in polarizability between the ground and excited states and m_f is the permanent dipole moment of the excited state (the ground state has no permanent dipole moment). The first term describes bleaching of the absorption due to transfer of oscillator strength from allowed to forbidden transitions ($c < 0$) and the last term in Eq. (1) (α') describes induced absorption.

For electroabsorption measurements, interdigitated aluminum electrodes with spacing 100 μm and thickness 50 nm were evaporated onto the spin-coated polymer films. This permitted the absorption spectrum of a film to be measured prior to electroabsorption measurements. It also permitted a film to be thermally cycled without damage to the electrodes. Electroabsorption samples were mounted in a liquid nitrogen cooled cryostat equipped with optical and electrical access. A 5000 Hz sinusoidal electric field was applied to the sample using the reference output of a lock-in amplifier driving a high voltage amplifier. Light from a 150 W xenon bulb is dispersed through a monochromator, focused onto the sample, and then onto a photodiode or photomultiplier tube. Lock-in amplification was employed to detect changes ΔT in the transmission T . The resulting spectra, to a good approximation, are proportional to the imaginary part of the dc Kerr susceptibility, $\text{Im}\chi^{(3)}(-\omega; \omega, 0, 0)$.

Photogeneration mechanisms and photoexcitation dynamics were studied by photoinduced absorption spectroscopy. This technique uses standard phase-sensitive lock-in techniques with a modulated Ar^+ laser beam as a pump and a broad spectrum light source as a probe. The PA spectrum, defined as the normalized change ΔT in the probe transmission T , is related to the photoexcitation density n by

$$-\Delta T/T = n\sigma d, \quad (2)$$

where σ is the excitation cross section and d the sample thickness. The PA signal is related to the excitation quantum yield η by

$$-\Delta T/T = \eta\tau\sigma, \quad (3)$$

where τ is the excitation lifetime and S the photon flux per unit area. The PAE spectrum is measured by varying the

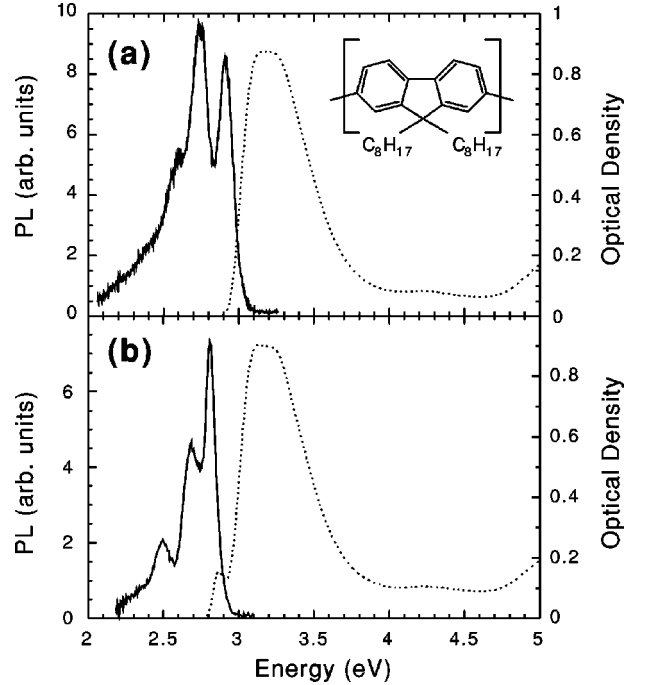


FIG. 1. (a) Absorption (dashed line) and PL (solid line) spectra of a spin-cast PFO film. Inset: chemical structure of PFO. (b) Absorption (dashed line) and PL (solid line) spectra of a thermally cycled PFO film.

excitation wavelength λ and is a measure of the excitation quantum yield as a function of the incident photon energy.^{14,15} The photocurrent action spectrum of a PFO film sandwiched between indium tin oxide and aluminum electrodes was also measured. The photocurrent action spectrum is defined as the number of photocarriers generated per absorbed photon in a device configuration and the spectrometer has been previously described.¹⁶

III. ELECTRONIC STRUCTURE OF PFO PHASES

Figure 1(a) shows the absorption and PL spectra of a PFO film spin cast from toluene solution. The absorption begins at 2.9 eV and reaches a peak at 3.23 eV. The lowest energy absorption band is 0.5 eV wide with no vibronic structure. The PL spectrum exhibits a clear vibronic structure with peaks at 2.92, 2.75, and 2.57 eV. The absorption spectrum redshifts by 12 meV upon cooling the sample from 300 to 80 K, but no new features are observed. The thermochromic effect is due to freezing out vibrational and librational modes of motion that can shorten the effective conjugation length.¹⁷ At low temperatures, the conjugation length increases and the absorption spectrum redshifts.

Figure 1(b) shows the absorption and PL spectra of a PFO film following cooling to 80 K and slow warming to 300 K. A new absorption band with clear vibronic structure is superimposed upon the original absorption spectrum and the PL spectrum redshifts by 0.1 eV. The main absorption has also redshifted by 10 meV. Figure 2 shows the absorption spectrum of the β phase, which was determined from the change in the absorption spectrum. No thermochromic shift of the β phase absorption spectrum was observed.

Interchain effects cannot account for changes in the ab-

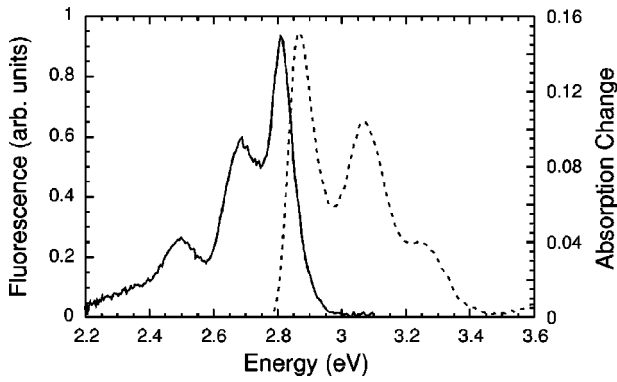


FIG. 2. Absorption spectrum of the β phase, determined by the change in the absorption spectrum of a PFO film upon thermal cycling. The fluorescence spectrum is also shown.

sorption and PL spectra of PFO upon thermal cycling. If the absorption peak at 2.86 eV were due to Davydov splitting of the main absorption band, there should be a corresponding blueshifted absorption peak and reduced fluorescence yield.¹⁸ J-aggregate formation causes significant narrowing of the absorption and emission spectra, whereas we observe only a redshift of 0.1 eV in the PL. Interchain aggregation can lead to excimer emission,^{19,20} which is characterized by a reduction of the PL quantum yield and a structureless PL that is redshifted by 0.5 eV or more with respect to the fluorescence.²¹ The lack of evidence for interchain effects supports the conjecture that the β phase is an intrachain state with extended conjugation.^{7,8}

We investigated the effects of β phase formation on the electronic structure of PFO by EA spectroscopy. The nonlinear optical properties of phenylene-based (π -conjugated) polymers are dominated by contributions from four essential states: the $1A_g$ (ground state), $1B_u$, mA_g , and nB_u states.^{22,23} Transient pump-probe measurements by Frolov *et al.* have shown that there is an additional even parity state strongly coupled to $1B_u$, which has been labeled the kA_g state.²⁴ Barford *et al.* have extended the essential four-state model to include the contributions of this state to the nonlinear optical properties of poly(*para*-phenylenes).²⁵

Figure 3(a) shows the EA spectrum of a glassy PFO film, measured at 77 K. The EA spectrum is dominated by two oscillatory features with zero-level crossings at 3.12 and 4.07 eV. The low energy feature is due to a Stark shift of the $1B_u$ exciton and the high energy feature to a combination of induced absorption by the mA_g state and a Stark shift of nB_u state. The latter feature is particularly important as the nB_u state is considered to lie close to the onset of the continuum band.²⁶ The solid line shows a fit to the EA spectrum, using Eq. (1). The contribution of the mA_g state is a Lorentzian centered at 4.03 eV and the contribution of nB_u is the derivative with respect to energy of a Lorentzian centered at 4.03 eV. From this fit, we have determined the polarizability difference between the $1A_g$ and $1B_u$ states, $\Delta p = 8.1 \times 10^{-19} \text{ eV m}^2/\text{V}^2$ (2300 \AA^3).

Both phases contribute to the EA spectrum of the thermally cycled sample, shown in Fig. 2(b). There is a new derivative-shaped feature with a zero-level crossing at 2.86 eV due to a Stark shift of the $1B_u$ state of the β phase. Induced absorption peaks are seen at 3.68 and 3.86 eV and

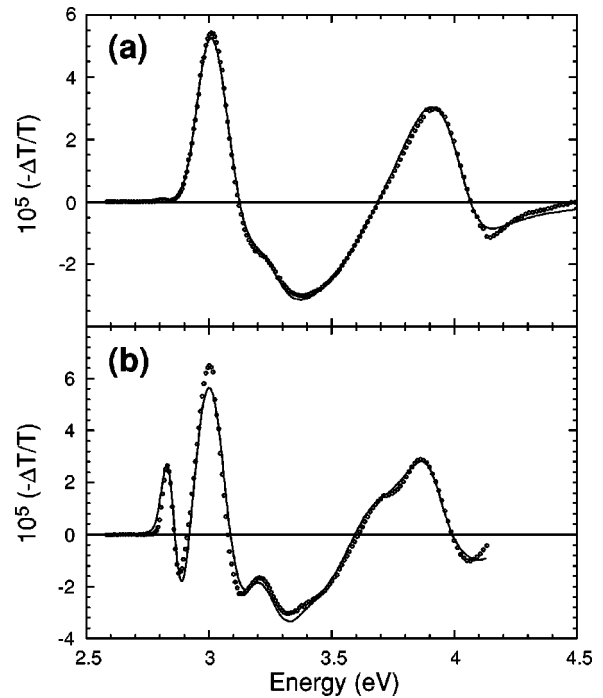


FIG. 3. (a) Circles: EA spectrum of amorphous PFO film. Line: Model of the EA spectrum. (b) Circles: EA spectrum of thermally cycled sample. Line: Model of the EA spectrum.

the zero-level crossing at 4.07 eV has redshifted to 4.01 eV. The polarizability of the β phase is nearly twice that of the glassy phase, $\Delta p = 1.5 \times 10^{-18} \text{ eV m}^2/\text{V}^2$ (4200 \AA^3), and therefore has a relatively larger contribution to the EA spectrum of the thermally cycled sample than to its absorption spectrum. Again, this is consistent with the β phase being a phase of polyfluorene with extended π conjugation. The solid line shows a fit to the EA spectrum, assuming independent contributions of the two phases to the EA spectrum. The energies of the mA_g and nB_u states have redshifted slightly, to 3.67 and 3.95 eV, respectively, and the induced absorption features are slightly narrower. Even though there is no thermochromic shift in β phase PFO, the polarizability at 437 nm measured by EA increases by 80%. The polarizability difference between the $1A_g$ and $1B_u$ states is apparently more sensitive to increased conjugation than is the optical gap.

IV. PHOTOEXCITATION DYNAMICS

The morphology of PFO films has a strong influence on photogeneration of polarons and triplet excitons. Figure 4 shows the PA spectrum of (a) the as-spun sample and (b) the thermally cycled sample. The PA spectrum of the as-spun sample is dominated by an unusually sharp and strong transition at 1.43 eV with a weak sideband at 1.62 eV. There was no evidence for photoinduced infrared active vibrations that accompany charged excitations.²⁷⁻²⁹ We accordingly assign the PA band at 1.43 eV to excited state absorption of triplet excitons. The full width at half maximum of this transition is 38 meV, the sharpest triplet excited state absorption feature ever observed for a conjugated polymer. A sharp transition accompanied by a relatively weak and broad vibronic sideband is characteristic of an optical transition where there is little geometric relaxation between the two states (the

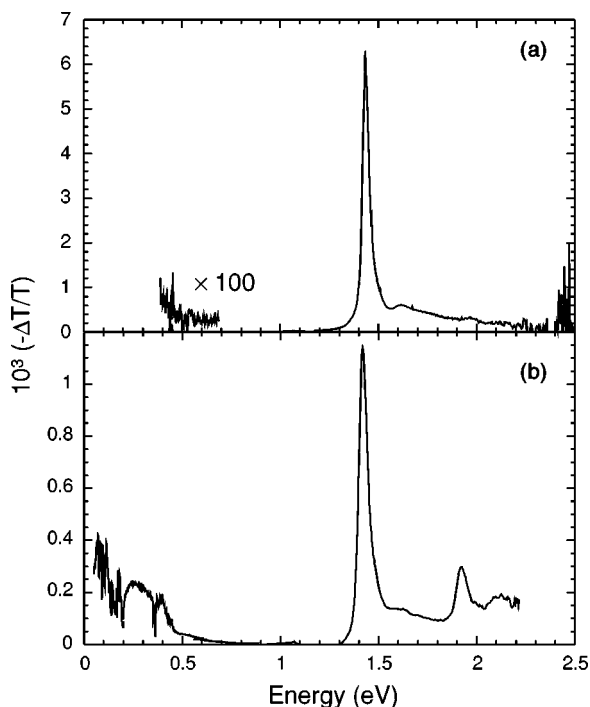


FIG. 4. (a) PA spectrum of an as-spun PFO film. (b) PA spectrum of a thermally cycled PFO film.

Huang-Rhys parameter $S \ll 1$). Such a narrow linewidth also requires there to be very little inhomogeneous broadening of the transition, indicative of a material with low energetic disorder. The PA spectrum continues up to 2.4 eV and PA below 1.4 eV is weak ($-\Delta T/T < 10^{-5}$).

The PA spectrum of the thermally cycled sample is shown in Fig. 4(b). The triplet PA band is eight times weaker than in the glassy sample and two new PA bands appear at 1.93 and 0.3 eV. These PA bands have the same dependence on pump power and modulation frequency and are accompanied by a series of sharp infrared active vibrations below 0.2 eV. The PA spectrum below 0.4 eV was measured using a Fourier transform infrared (FTIR) spectrometer and is shown on an expanded scale in Fig. 5. All of these results are characteristic of polarons, charged excitations with spin 1/2. The assignment was confirmed by PA-detected magnetic resonance (PADMR) measurements.³⁰ We accordingly assign these PA bands to transitions of polarons. Comparison of the

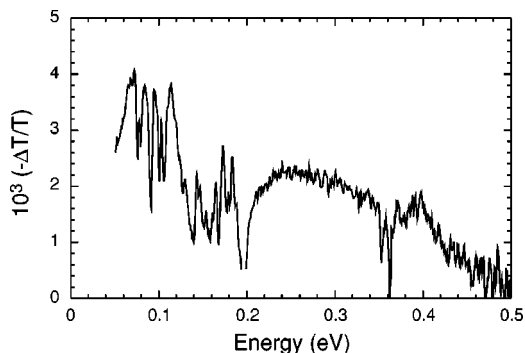


FIG. 5. The low energy portion of the PA spectrum of a thermally cycled PFO film, showing photoinduced infrared active vibrations.

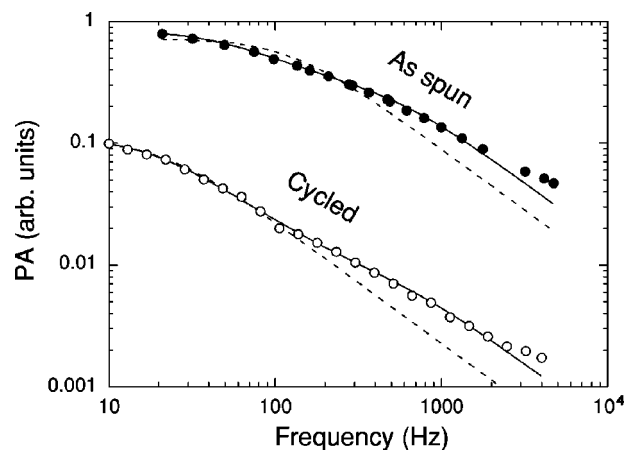


FIG. 6. Dependence of the triplet PA upon the modulation frequency. The as-spun sample is shown as filled circles, the thermally cycled sample as open circles. Fits to the frequency dependence using one or two lifetimes are shown as dashed and solid lines, respectively.

PA below 0.5 eV of the two samples shows that the polaron yield is approximately 10 to 15 times stronger in the thermally cycled sample than in the as-spun sample. There is a weak feature at 1.95 eV in the PA spectrum in Fig. 4(a) and the polaron could be clearly detected in the PADMR spectrum of an as-spun sample.³⁰

The frequency dependence of the triplet PA for both samples is shown in Fig. 6. The triplet PA depends linearly on the excitation power, indicating monomolecular recombination kinetics. For monomolecular recombination kinetics, the magnitude of the PA depends upon the modulation frequency as

$$\Delta T \propto 1/\sqrt{1 + (2\pi f\tau)^2}, \quad (4)$$

where f is the modulation frequency and τ is the excitation lifetime. The decay of the triplet PA signal with increasing frequency could not be well fitted to a single excitation lifetime (dashed lines), but could be fitted with a biexponential decay (solid lines). The triplet lifetime of the as-spun sample is 1.8 ms with a 13% fraction of triplets having a lifetime of 98 μ s. The triplet lifetime of the thermally cycled sample is slightly longer (7.4 ms) with a 2.5% fraction of triplets having the shorter lifetime (93 μ s). We can also estimate the triplet quantum yield in glassy phase PFO to be 5%, assuming a similar cross section for triplet excitons as for excited state absorption of singlet excitons in a substituted PPV [$\sigma_T = 1.8 \times 10^{-15} \text{ cm}^2$ (Ref. 31)] and using Eq. (2). The high fluorescence quantum yield of PFO (50%) puts a lower limit on the triplet cross section: $\sigma_T \geq 2.0 \times 10^{-16} \text{ cm}^2$.

The narrow PA band triplet excitons and the fact that polarons are generated only in the β phase provide a unique opportunity to compare different photogeneration mechanisms of triplet excitons in π -conjugated polymers. The most direct method to produce triplet excitons is intersystem crossing of singlet excitons. Like fluorescence, intersystem crossing will follow thermalization of singlet excitons and should be independent of the pump photon energy.^{15,34} Triplet excitons may also be indirectly photogenerated through recombination of photogenerated polarons. Spin statistics

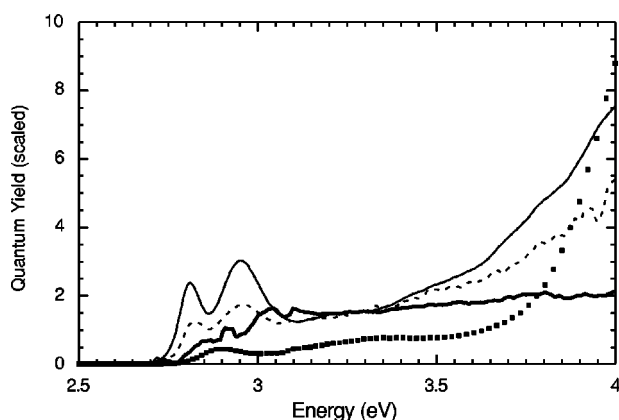


FIG. 7. The PAE spectra for triplet excitons in an as-spun PFO film (bold line), triplet excitons (solid line), and polarons (dashed line) in a thermally cycled film. The photocurrent action spectrum is shown as symbols for comparison.

predicts a 75% yield of triplet excitons from recombination of nongeminate polaron pairs, although singlet formation rates as high as 50% have been proposed.^{35,36} Frankevich and co-workers have proposed that evolution of the spin state of long-lived geminate polaron pairs can also result in the production of triplet excitons.³⁷ For production of triplet excitons from polaron pairs, the triplet and polaron PAE spectra should resemble each other. The polaron PAE spectrum in π -conjugated polymers typically has a step at the onset of absorption followed by a marked increase in the polaron yield for pump energies 0.6–1.0 eV above the absorption edge.

Figure 7 shows the PAE spectra of triplet excitons in an as-spun film, measured at 1.43 eV, and of triplet excitons and polarons, measured at 1.93 eV, in a thermally cycled sample. Triplet excitons contribute approximately 20% of the PA at 1.93 eV in the thermally cycled sample. The PAE spectrum of the as-spun film, due to triplet excitons, has an onset at the absorption onset and increases only slightly as the photon energy increases. The weak dependence on photon energy is consistent with direct intersystem crossing of singlet excitons. As charge photogeneration is extremely weak in this film, intersystem crossing should be the dominant photogeneration mechanism for triplet excitons.

The PAE spectra of both polarons and triplet excitons in the thermally cycled sample are quite different. The onset of the PAE spectrum of the thermally cycled sample is close to the β phase absorption and has local maxima at 2.81 and 2.96 eV. The polaron quantum yield steadily increases as the photon energy increases. This is characteristic of intrinsic charge photogeneration, where exciton dissociation proceeds directly upon creation of a “hot” exciton.^{33,15,32} The PAE spectra resemble the photocurrent action spectrum of PFO, shown as symbols in Fig. 7, as well as the polaron PAE spectrum of methyl-substituted LPPP.¹⁵ The differences in the polaron yields of the two films suggest a possible relation between the effective conjugation length and photocarrier yield. For a sample with conformationally limited conjugation length, intrinsic charge photogeneration is weak and charge photogeneration is dominated by extrinsic (defect-related) mechanisms. The line shape of the triplet PAE spectrum of the thermally cycled sample is quite different from

that of the as-spun sample, but follows the polaron PAE spectrum. Thus, our results show a clear link between triplet and charge photogeneration. Additional studies of the two types of PFO film should further clarify the link between these two long-lived photoexcitations.

There is a striking similarity in the optical properties of β phase PFO and LPPP. The absorption and PL spectra are displaced only 50 meV relative to one another, have similar vibronic progressions, and both β phase PFO and LPPP have small Stokes shifts³⁸ between the 0-0 absorption and PL peaks (70 meV and 60 meV, respectively). Furthermore, the optical transitions of triplet excitons and polarons occur at nearly the same energies in both materials.^{15,19,38–43} In view of these similarities, it is surprising that a study comparing LPPP and several of its oligomers concluded that LPPP has a much shorter conjugation length (10–14 phenyl rings) than PFO or other *para*-phenylene polymers;⁴⁴ this despite the fact that the molecular design of LPPP forces a coplanar conformation of all conjugated units. This conclusion is further contradicted by the redshifted absorption and fluorescence spectra of LPPP in comparison to the dialkoxy-substituted PPP derivative, poly(2,5-diheptyloxy-1,4-phenylene).^{45,46} Rather, the rapid convergence of the optical transitions of LPPP oligomers with those of the polymer suggests that excitons in LPPP are self-localized. Therefore, the coherence length of planarized LPPP is much larger than the exciton size dimensions. These results would also indicate that conjugation lengths calculated from series of oligomers of most conjugated polymers results in a conformationally limited estimate of the conjugation length.

V. CONCLUSIONS

In summary, we found that an additional solid phase, the β phase, is formed in PFO films upon thermal cycling from 80 to 300 K. This phase consists of polymer chains with extended π conjugation. Compared to glassy samples prepared by spin casting from solution, excitations of the β phase are redshifted and have a higher polarizability. PA and PAE measurements show that polarons are more easily formed in the β phase and that there is a clear link between polaron and triplet photogeneration.

ACKNOWLEDGMENTS

We would like to thank the Dow Chemical Company for supplying the polyfluorene samples studied in this work. Research performed at the University of Sheffield was supported in part by the U.K. Engineering and Physical Sciences Research Council (Grant No. GR/L80775) and the Royal Society (Grant No. RS19025). Research performed at the University of Utah was supported by the U.S. Department of Energy under Grant No. DOE FG-03-96 ER 45490. The collaboration between Sheffield and the University of Utah was supported by NATO Collaborative Research Grant No. CRG 973132.

- ¹A. Grice, D. D. C. Bradley, M. T. Bernius, M. Inbasekaran, W. Wu, and E. P. Woo, *Appl. Phys. Lett.* **73**, 629 (1998).
- ²M. Redecker, D. D. C. Bradley, M. Inbasekaran, and E. P. Woo, *Appl. Phys. Lett.* **73**, 1565 (1998).
- ³M. Grell, D. D. C. Bradley, M. Inbasekaran, and E. P. Woo, *Adv. Mater.* **9**, 798 (1997).
- ⁴M. Grell, W. Knoll, D. Lupo, A. Meisel, T. Miteva, D. Neher, H. G. Nothofer, U. Scherf, and A. Yasuda, *Adv. Mater.* **11**, 671 (1999).
- ⁵M. Redecker, D. D. C. Bradley, M. Inbasekaran, and E. P. Woo, *Appl. Phys. Lett.* **74**, 1400 (1999).
- ⁶M. N. Shkunov, R. Österbacka, A. Fujii, K. Yoshino, and Z. V. Vardeny, *Appl. Phys. Lett.* **74**, 1648 (1999).
- ⁷M. Grell, D. D. C. Bradley, X. Long, T. Chamberlain, M. Inbasekaran, E. P. Woo, and M. Soliman, *Acta Polym.* **49**, 439 (1998).
- ⁸M. Grell, D. D. C. Bradley, G. Ungar, J. Hill, and K. S. Whitehead, *Macromolecules* **32**, 5810 (1999).
- ⁹G. Klaerner and R. D. Miller, *Macromolecules* **31**, 2007 (1998).
- ¹⁰N. Miyaura and A. Suzuki, *Chem. Rev.* **95**, 2457 (1995).
- ¹¹M. Bernius, M. Inbasekaran, E. Woo, W. S. Wu, and L. Wujkowski, *Proc. SPIE* **3621**, 93 (1999).
- ¹²S. Janietz, D. D. C. Bradley, M. Grell, C. Giebeler, M. Inbasekaran, and E. P. Woo, *Appl. Phys. Lett.* **73**, 2453 (1998).
- ¹³L. Sebastian and G. Weiser, *Phys. Rev. Lett.* **46**, 1156 (1981).
- ¹⁴P. A. Lane, M. Liess, J. Partee, J. Shinar, A. J. Frank, and Z. V. Vardeny, *Chem. Phys.* **227**, 57 (1998).
- ¹⁵M. Wohlgenannt, W. Graupner, G. Leising, and Z. V. Vardeny, *Phys. Rev. Lett.* **82**, 3344 (1999).
- ¹⁶C. Giebeler, R. N. Marks, A. Bleyer, D. D. C. Bradley, and S. Schrader, *Opt. Mater.* **9**, 99 (1998).
- ¹⁷T. W. Hagler, K. Pakbaz, K. F. Voss, and A. J. Heeger, *Phys. Rev. B* **44**, 8652 (1991).
- ¹⁸M. Pope and C. E. Swenberg, *Electronic Processes in Organic Crystals* (Oxford University Press, New York, 1982).
- ¹⁹G. Cerullo, S. Stagira, M. Nisoli, S. De Silvestri, G. Lanzani, G. Krangelbinder, W. Graupner, and G. Leising, *Phys. Rev. B* **57**, 12 806 (1998).
- ²⁰U. Lemmer, S. Heun, R. F. Mahrt, U. Scherf, M. Hopmeier, U. Siegner, E. O. Gobel, K. Müllen, and H. Bassler, *Chem. Phys. Lett.* **240**, 373 (1995).
- ²¹S. A. Jenekhe and J. A. Osaheni, *Science* **265**, 765 (1994).
- ²²D. Guo, S. Mazumdar, S. N. Dixit, F. Kajzar, F. Jarka, Y. Kawabe, and N. Peyghambarian, *Phys. Rev. B* **48**, 1433 (1993).
- ²³S. J. Martin, D. D. C. Bradley, P. A. Lane, H. Mellor, and P. L. Burn, *Phys. Rev. B* **59**, 15 133 (1999).
- ²⁴S. V. Frolov, M. Liess, P. A. Lane, W. Gellerman, Z. V. Vardeny, M. Ozaki, and K. Yoshino, *Phys. Rev. Lett.* **78**, 4285 (1997).
- ²⁵W. Barford, R. J. Bursill, and M. Y. Lavrentiev, *J. Phys.: Condens. Matter* **10**, 6429 (1998).
- ²⁶M. Chandross and S. Mazumdar, *Phys. Rev. B* **55**, 1497 (1997).
- ²⁷D. Moses, A. Dogariu, and A. J. Heeger, *Chem. Phys. Lett.* **316**, 356 (2000).
- ²⁸D. Moses, A. Dogariu, and A. J. Heeger, *Phys. Rev. B* **61**, 9373 (2000).
- ²⁹U. Mizrahi, I. Shtrichman, D. Gershoni, E. Ehrenfreund, and Z. V. Vardeny, *Synth. Met.* **102**, 1182 (1999).
- ³⁰A. J. Cadby, P. A. Lane, S. Martin, D. D. C. Bradley, M. Wohlgenannt, C. An, and Z. V. Vardeny, *Synth. Met.* **111-112**, 515 (2000).
- ³¹W. Holzer, A. Penzkofer, S. H. Gong, D. D. C. Bradley, X. Long, and A. Bleyer, *Chem. Phys.* **224**, 315 (1997).
- ³²V. I. Arkhipov, E. V. Emelianova, and H. Bässler, *Phys. Rev. Lett.* **82**, 1321 (1999).
- ³³S. Barth and H. Bässler, *Phys. Rev. Lett.* **79**, 4445 (1997).
- ³⁴This assumption neglects the possibility of higher intersystem crossing rates for different absorption bands (upper excited state transfer).
- ³⁵Y. Cao, I. D. Parker, G. Yu, C. Zhang, and A. J. Heeger, *Nature (London)* **397**, 414 (1999).
- ³⁶Z. Shuai, D. Beljonne, R. J. Silbey, and J. L. Bredas, *Phys. Rev. Lett.* **84**, 131 (2000).
- ³⁷E. L. Frankevich, A. A. Lymarev, I. Sokolik, F. E. Karasz, S. Blumstengel, R. H. Baughman, and H. H. Horhold, *Phys. Rev. B* **46**, 9320 (1992).
- ³⁸W. Graupner, M. Mauri, J. Stampfl, O. Unterweger, and G. Leising, *Mol. Cryst. Liq. Cryst. Sci. Technol., Sect. A* **256**, 431 (1994).
- ³⁹W. Graupner, M. Mauri, J. Stampfl, G. Leising, U. Scherf, and K. Müllen, *Solid State Commun.* **91**, 7 (1994).
- ⁴⁰W. Graupner, S. Eder, K. Petritsch, G. Leising, and U. Scherf, *Synth. Met.* **84**, 507 (1997).
- ⁴¹K. Petritsch, W. Graupner, G. Leising, and U. Scherf, *Synth. Met.* **84**, 625 (1997).
- ⁴²W. Wohlgenannt, W. Graupner, G. Leising, and Z. V. Vardeny, *Phys. Rev. B* **60**, 5321 (1999).
- ⁴³E. J. W. List, J. Partee, J. Shinar, U. Scherf, K. Müllen, E. Zojer, K. Petritsch, G. Leising, and W. Graupner, *Phys. Rev. B* **61**, 10 807 (2000).
- ⁴⁴J. Grimme, M. Kreyenschmidt, F. Uckert, K. Müllen, and U. Scherf, *Adv. Mater.* **7**, 292 (1995).
- ⁴⁵M. Hamaguchi and K. Yoshino, *Jpn. J. Appl. Phys., Part 2* **34**, L587 (1995).
- ⁴⁶Z. V. Vardeny, P. A. Lane, M. Liess, H. Hamaguchi, M. Ozaki, and K. Yoshino, *Synth. Met.* **84**, 641 (1997).